[redacted] UNCLASSIFIED

LA-718

[redacted]

17 December 1948

This document contains 51 pages.

ENERGY SPECTRUM OF NEUTRONS FROM FISSIONS INDUCED BY THERMAL NEUTRONS

Work done by:

B. E. Watt

Report written by:

B. E. Watt

[redacted] UNCLASSIFIED

ABSTRACT

A proton recoil counter has been used to determine the neutron spectrum, in the energy range 3.3 → 17 Mev, of a beam produced by irradiating 95% U^{235} (metal) in the glory hole of the water boiler: most of the fissions were induced by slow neutrons. The data obtained are believed to represent the fission spectrum, and are combined with data obtained by D. Hill and by T. W. Bonner, R. A. Ferrell, and M. C. Rinehart: the composite spectrum so obtained extends from 0.075 to 17 Mev.

Fits with two general formulas are discussed.

ENERGY SPECTRUM OF NEUTRONS FROM FISSIONS INDUCED BY THERMAL NEUTRONS

Introduction

Previous experiments to determine the neutron spectrum yielded little information at energies higher than 6 Mev, and the data at low energies disagreed rather surprisingly with any reasonable theory.

In view of the importance for design, and the interest in the intensity at 15 Mev, special emphasis was laid on the high energy portion of the spectrum: a very intense, well collimated beam of neutrons could be obtained from the "water boiler", so made investigation of the high energy portion of the spectrum particularly attractive.

Several methods for observing the spectrum were considered, and the proton recoil method chosen because the factors necessary to compute the neutron spectrum were well known.

Apparatus

The neutron beam was produced by inserting samples of U^{235} (95.1%) in the "glory hole" of the water boiler, where they were exposed to a thermal neutron flux of 3×10^{11} per square centimeter. Two such sources were used: (1) a 28.5 gram disk of U^{235} 0.168 inch thick mounted on a graphite rod, and (2) an assembly of 31 disks 0.010 inch thick equally spaced along an 18 inch aluminum tube: the

total mass of U^{235} was 54.1 grams.

Since the presence of such large amounts of active material materially alters the neutron distribution in the reactor, and since samples thicker than about 0.015 inch absorb essentially all the slow neutrons incident on them, the fission rate in the source is not directly proportional to the amount of active material. A better measure is the "effective mass", defined as the amount of material which, when dissolved in the reactor's solution, would give the same increase in reactivity as does the sample when placed in the glory hole. By this definition, the effective mass of the 28.5 gram disk was 6.1 grams, and the effective mass of the 31 disk source was 42.6 grams; from these measurements, the multiple disk source was expected to produce a beam approximately seven times as strong as that from the single disk source, a conclusion borne out by the spectrometer measurements. Unfortunately, the average fission rate per gram throughout the reactor is not the same as the average fission rate per gram of either the actual or the effective mass of the source used, so only rough comparison between the observed and expected number of neutrons is possible.

As the primary objective of the experiment was to determine the shape of the fission spectrum, it was necessary to consider the effect of scattering in the walls of the collimating tube. A very crude calculation considering only

[redacted]

single scattering indicated that less than 1% of the emerging beam had been scattered in the walls. Since the most objectionable feature of such scattering is distortion of the spectrum through degradation, and since an energy loss of 3 Mev would put neutrons observed in this experiment into a group about ten times as strong as the parent group, it is believed that wall scattering is negligible in this experiment.

Many factors contributed to the design of the spectrometer, some of which are mentioned below: a cross section of the apparatus is shown in Fig. 1 and the experimental set-up is sketched in Fig. 2. It was known that the intensity of the very high energy neutrons would be low, therefore the apparatus was designed to operate stably for long periods. The three proton counters were removed from the neutron beam in order to reduce their singles counting rate and therefore the background; no moving parts of any kind were placed in them to reduce the probability of a change in the counter characteristics. The values given below are those used for the determination of the fission spectrum and are, in a few instances, different from those used to determine the spectrum produced by the 28.5 gm disk. The recoil protons were ejected from any one of four polyethylene foils, passed through any desired combination of seven aluminum absorbers and the one mil (7.91 mg/cm^2)

[redacted]

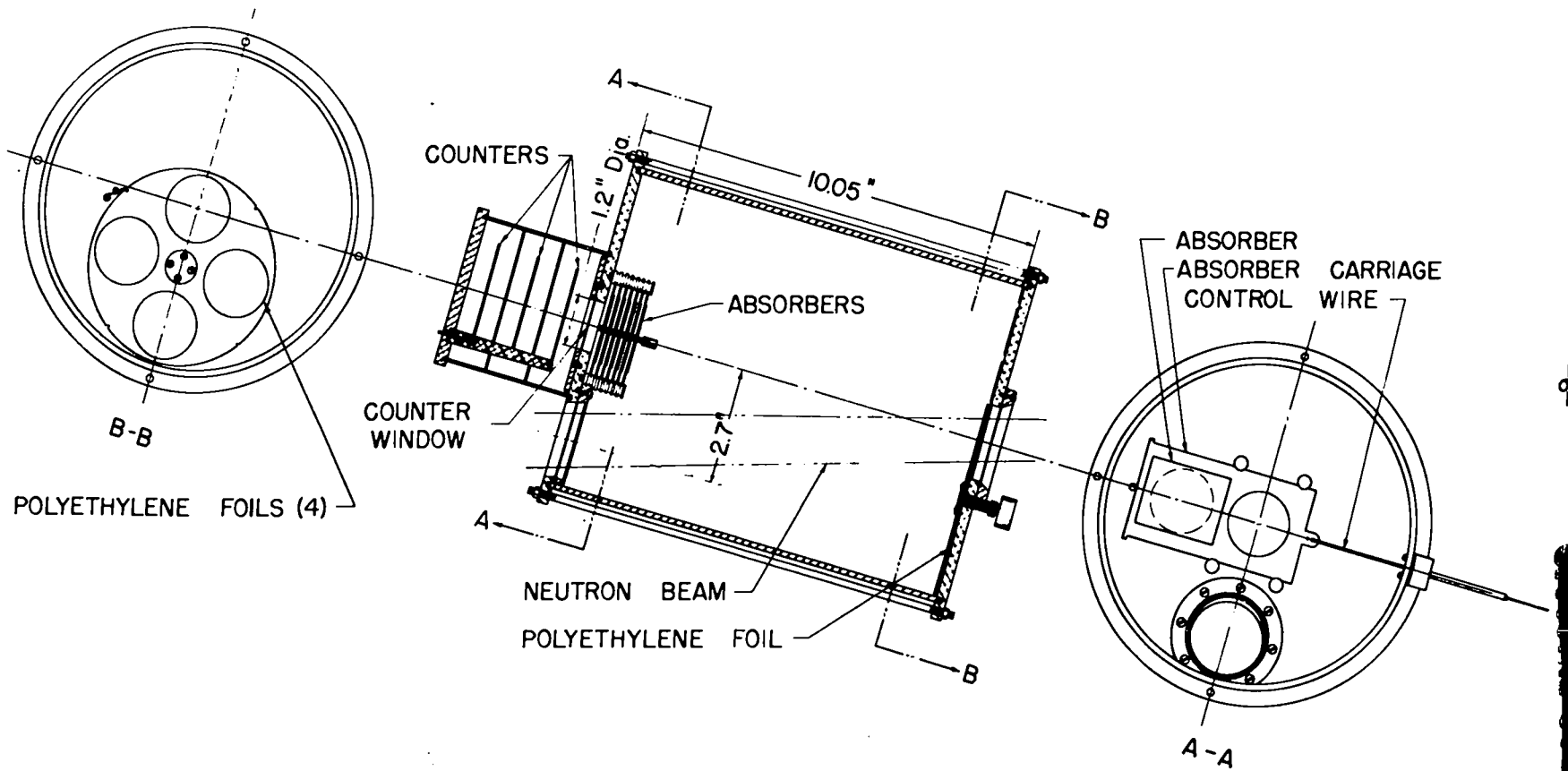

FIG 1

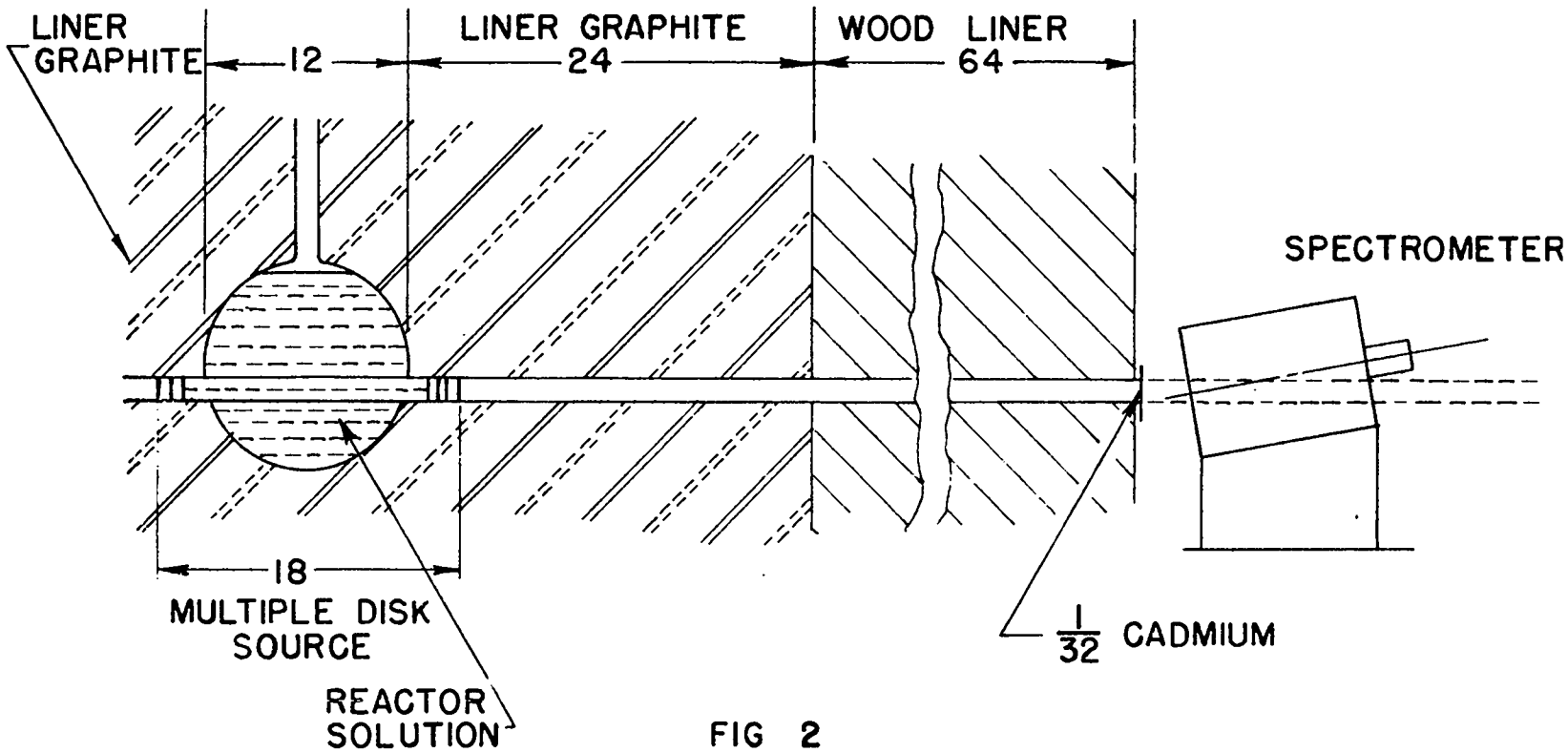

FIG 2

APPROVED FOR PUBLIC RELEASE

[redacted]

Duralumin foil covering the 1.2 inch aperture for the counters. The thicknesses of the polyethylene foils and aluminum absorbers are listed in Tables I and II, respectively. Each counter was made one inch deep in order to get a large ion pulse, comparable with the pulses from argon recoils and larger than beta ray pulses, and to reduce the number of alpha particles which could give triple coincidences. The counters were operated as proportional amplifiers with a gas filling of 5% CO_2 and 95% of 99.8% pure tank argon at a total pressure of 22 inches of mercury. Over a period of a month, the counting rate vs. voltage curves shifted to higher voltage by about five percent, but no other change was noted. The singles counting rate of #3 counter was used to check continuously the proper performance of all counters: the triple coincidence counting rates taken on different days agreed within the statistical uncertainty about one percent, therefore it is believed that no errors were introduced by shifts in the counter characteristics.

The entire a.c. supply was obtained through a radio-frequency filter to remove possible pulses on the line, then stabilized with a Sorenson Model 1000 voltage stabilizer. During a week's run, the high voltage supply for the counters, also electronically regulated, was not observed to vary by twenty volts. The pulses from each counter were amplified by a Model 100 amplifier and clipped with a 200

[redacted]

[redacted]

TABLE I

Polyethylene foil thicknesses

Poly Number	Thickness (t) mg/cm^2	Range equivalent in aluminum mg/cm^2
2	2.06	2.88
3	5.70	7.96
4	21.01	29.35
1	71.88	100.4

TABLE II

Aluminum absorber thicknesses

Absorber	Thickness
Counters	7.1 ± 1*
Counter window	$7.91 \pm .03$
1	$6.39 \pm .03$
2	$13.04 \pm .05$
3	$27.0 \pm .1$
4	$42.2 \pm .2$
5	$110.4 \pm .4$
6	$215.8 \pm .9$
7	216

* see text

[redacted]

micro-microfarad condenser, giving output pulses a few microseconds wide. It was found necessary to add grid current limiting resistors to improve the overload characteristics of the amplifiers. The amplified pulses fed a triple coincidence circuit, and the number of coincidences was recorded with a Model 200 scale of 64. A second scale of 64 recorded the amplified pulses from counter #3 which could contribute to the triple coincidences. Owing to the slightly different geometry of the center counter, it was necessary to reduce the voltage applied to the counters #1 and #3 by 9% in order to obtain the same gas amplification in each counter. The counting rate vs. voltage curves are shown in Fig. 3.

If the counters should operate primarily as differential counters the proton distribution observed would be wrong because of the systematic change in the specific ionization, therefore energy range contributing to the count. The shape of the counting rate vs. voltage curves indicated no such effect, but as a check the ratio of neutron intensities observed with 2250 and 2450 volts applied to the counters was computed. At 3.2 Mev the ratio was 1.16 ± 0.02 and at 9.7 Mev the ratio was 1.19 ± 0.1: from these ratios, it was concluded that the relative intensities of the high and low energy portion of the spectrum are probably correct within 15%.

By reducing the gains of each channel's amplifier

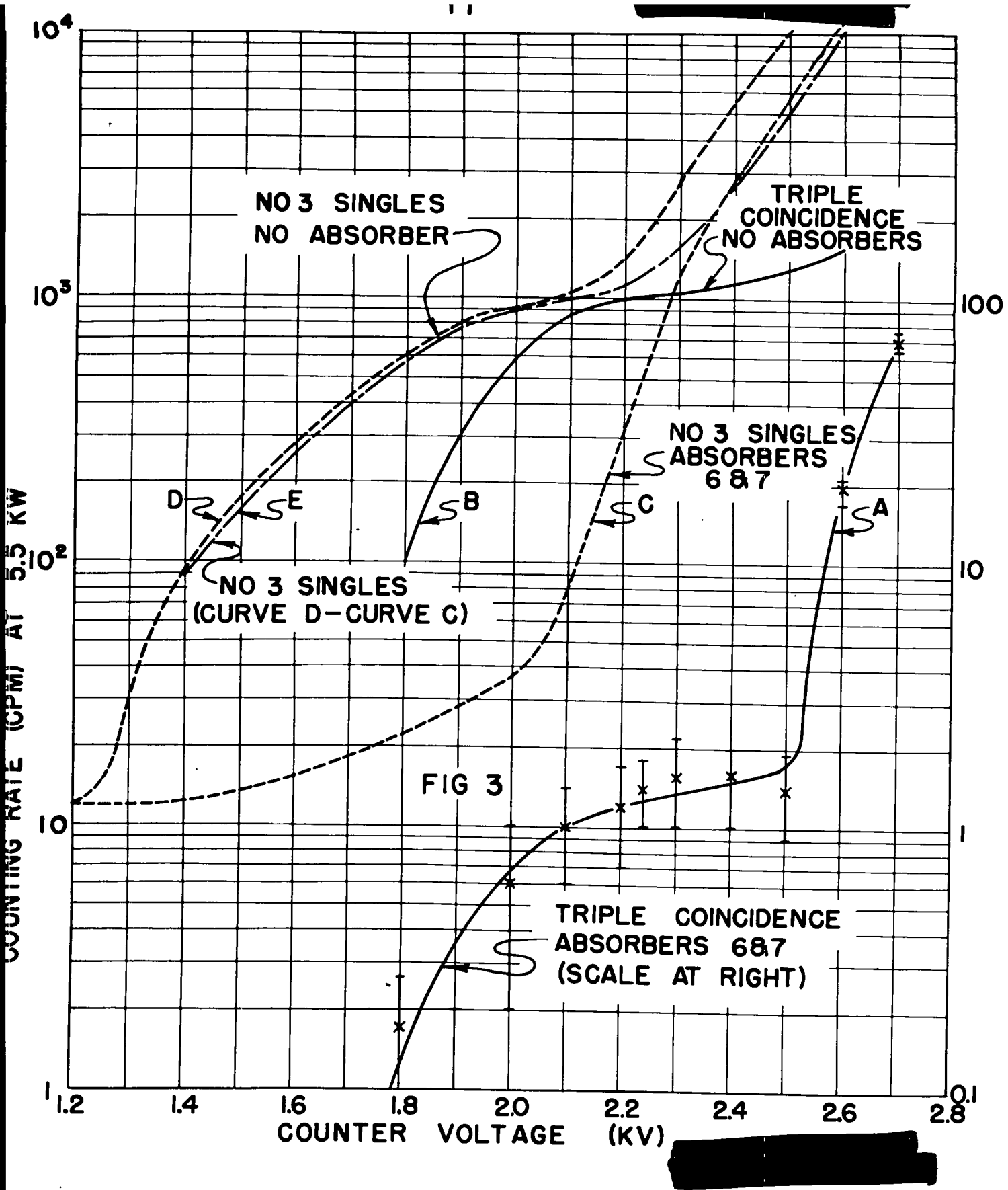

FIG 3

a factor of four and repeating the counting rate vs. voltage curve, it was found that increasing the applied voltage 400 volts increased the gas amplification a factor of 4. Then the increase from 2250 to 2450 volts resulted in a reduction of a factor of 2 in the energy loss necessary in the counters, so was an adequate check that the counters were not operating as differential counters.

The insertion of absorbers #6 and #7 completely removed the protons and electrons originating in the polyethylene foil or adjacent materials, but didn't appreciably change the neutron flux anywhere in the apparatus. The difference between the counting rates with no absorber and with absorbers #6 and #7 in place should be due to protons alone, assuming no counts from electrons knocked on by the rather intense gamma beam accompanying the neutrons.

The counting rate vs. total applied voltage for the triple coincidences of the three counters and the single pulses in counter #3 are shown in Fig. 3 for the two cases (1) no absorbers and (2) absorbers #6 and #7 in place. The difference between the two curves is ascribed to charged particles originating near the polyethylene foils; the exponential rise in the difference curve for #3 singles can't be ascribed to protons, and it is difficult to see how the slight change in the positions of the absorbers could change the number of argon recoils by a factor of two. If, however,

the exponential rise in the singles rate is due primarily to electrons ejected by the gamma rays such a rise in the difference could be explained. The maximum energy loss possible for an electron in the gas of any one counter was about 80 kev, so they could not be dismissed as agents for producing counts. Electrons penetrating all the counters could give triple coincidences, and the effect of the absorbers would be very different from that produced on the proton count. An electron passing through the counters normal to the planes of the collecting grids could lose a maximum of 34 kev in, say, #3 counter, 17 kev in #2 and 14 kev in #1. As the total amplifications of the three channels were essentially the same, then the increase of gas amplification observed implies that about 250 volts above the point where such electrons begin to count in #3 counter beta rays could produce a triple coincidence. Inspection of the curves in Fig. 3 shows an upward trend for the coincidence rate with no absorbers and a sharp break in the triple coincidence rate with absorbers #6 and #7 in place, both at about 2600 volts, while the exponential rise in the singles rate starts at about 2100 volts. The increase of gas amplification between these two voltages is computed to be a factor 5.7: if an 80 kev energy loss in #3 produced a singles count at 2100 volts, then a 14 kev energy loss produced a count at 2600 volts and a triple coincidence could be effected by a beta ray.

[redacted]

The considerations above seem to set a lower bound to the energy loss necessary to produce a count in the range 40 - 80 kev, for the operating condition of 2250 volts applied to the counters. Since the proton counting efficiency approaches unity at 2250 volts, the upper bound must lie in the range below 0.3 Mev. The spread in pulses owing to different paths through the counters may then be inferred as about a factor of five: though considerably larger than expected from the original design data, such a factor is quite believable in view of the rather slow rise at the start of the proton plateau.

Calculations

The minimum possible path within the counters necessary to produce a triple coincidence was 5.1 cm, the maximum possible path was 7.6 cm, and the mean value was 6.3 cm. In computing the range equivalent of the counters, the value 6.3 cm was used; the maximum error was 1 cm. At the operating pressure of 22 inches of mercury and with the 7.91 mg/cm^2 Duralumin window, the minimum proton range capable of producing a triple coincidence was 15 ± 1 mg/cm^2, corresponding to an energy of $2.45 \pm .1$ Mev. At the higher energies, the maximum error is less (0.05 at 5 Mev). From the counter's characteristics, it is believed that the probable error is less than 0.05 Mev at the lowest energy, and correspondingly lower at the higher energies.

[redacted]

[redacted]

From the atomic stopping powers it was computed that 1 mg/cm^2 of $(CH_2)_x$ was equivalent to 1.40 mg/cm^2 of aluminum. From the thicknesses of the polyethylene foils and aluminum absorbers, and the equivalent thickness of the counters and their window, the average minimum range of a proton giving a triple coincidence was computed. The range was then converted to proton energy by the range-energy relation computed by J. H. Smith, Phys. Rev. 71, 32 (1947). The energy difference between particular combinations of absorbers was also computed from the same data, but could be used only when the polyethylene foil was not simultaneously changed. The range-energy relation used is given in Appendix I.

Calculation of the neutron distribution from the observed counting rates.

It was convenient to define the following quantities:

C_p = proton counting rate = number of protons/min penetrating the counters;

E_p = proton energy;

E_n = neutron energy;

P = water boiler power level, kilowatts (proportional to source strength);

E_o = average minimum proton energy;

σ_s = total proton scattering cross section, barns;

$(t\rho)$ = polyethylene foil thickness, mg/cm^2.

[redacted]

The cross sections used were obtained from the theoretical curves of Bohm and Richman, Phys. Rev. 71,570 (1947) and Louis Goldstein (LA-702). The curve developed by Bohm and Richman fits the data of Bailey, Bennett, Bergstrahl, Nuckolls, Richards and Williams, Phys. Rev., 70, 583, (1946) quite well in the energy range 0.4 to 6 Mev. The curve developed by Goldstein fits the data of R. Sherr, Phys. Rev., 68,240 (1945) and W. Sleator, Jr., Phys. Rev., 72,207 (1947) in the energy range 9 to 23 Mev. However, "reasonable extrapolations" into the gap can't be made to join. A smooth curve was constructed by drawing a rather arbitrary join meeting Bohm and Richman's curve at 4 Mev and Goldstein's curve at about 14 Mev, as shown in Fig. 11. Acceptable joins could be made which differed by ten percent, so systematic errors of the order 5% at 8 Mev are to be expected. The values used are listed in Appendix II.

The complete derivations used to compute the neutron distribution are given in Appendix III. The resulting formulas are:

$$\overline{N(E_n)} = 3.04 \times 10^6 \ \Delta(C_p/Pt\rho)/\sigma_s \Delta E_o \qquad (1)$$

$$0.93\, E_n = E_p \qquad (2)$$

In order to preserve the accuracy of the difference $\Delta(C_p/Pt\rho)$, the values of ΔE_o were chosen to be about 1 Mev. Since the function $(N(E_n))$ falls by more than

a factor of two in such a large interval, it was thought desirable to plot the average value obtained at the energy where $N(E_n)$ would take on the average value. Since the function is nearly exponential in the energy range considered, the relation between energy interval width and plotting position is readily established. The result is a minor correction and is developed in Appendix IV.

Results

The first spectrum observed was that of a beam produced by a 28.5 gram disk of U^{235} 0.168 inch thick mounted on a graphite rod and placed in the center of the water boiler. The spectrum obtained is given in Table III, and could be fitted with the empirical equation

$$N(E_n) = 4.05 \times 10^6 \, P \, e^{-E_n/1.16} \qquad (3)$$

$$3 \leq E_n \leq 12 \text{ Mev}$$

It became evident that the above data could not yield the desired fission spectrum because (1) the intensity was too low to reach 15 Mev and (2) the number of neutrons produced in the reactor's solution and subsequently scattered into the beam by the walls of the collimating tube and the graphite rod backing constituted about a third of the total beam.

A new source was designed to reduce the amount of material capable of scattering neutrons from the reactor

[redacted]

TABLE III

E_n	$N(E) \times 10^{-4}$ neutrons/Mev (kw) sec
2.96	30.0 ±.8
4.17	9.67 ±.5
5.27	4.77 ±.4
6.25	1.63 ±.3
7.26	0.9 ±.1
8.50	0.33 ±.03
9.72	0.15 ±.03
10.69	0.04 ±.01
11.75	0.022 ±.007
12.73	0.020 ±.007

[redacted]

into the beam and to raise the beam intensity as much as possible. The design chosen was 31 disks of U^{235} 0.010 inch thick equally spaced along an 18" aluminum tube. The neutrons produced in the disk farthest from the spectrometer passed through 0.3 inch of uranium, so the distortion produced by self absorption in the source was negligible.

Three minor changes were made in the spectrometer while the multiple disk source was being designed and constructed: (1) the number 1 position of the polyethylene foil wheel was covered with a thick (71.88 mg/cm^2) foil; (2) the pure aluminum counter window (6.57 mg/cm^2) was replaced with the Duralumin window (7.91 mg/cm^2); and (3) the counters were operated at 22 inches of mercury pressure instead of 15. The values used for the determination of the spectrum of the beam from the open hole and the beam from the multiple disk source are given in the section on Apparatus.

The data obtained with the multiple disk source is given in Table IV, and the values of factors used in the computation together with the computed spectrum are listed in Table V.

The spectrum of the beam produced when the glory hole was empty was measured and the result listed in Table VI. The data can be fitted reasonably well with the equation

$$N(E_n) = 5.5 \times 10^5 \, P \, e^{-E/1.3} \qquad (4)$$

$$3 \leqslant E_n \leqslant 10$$

TABLE IV

Poly	Absorbers	$E_{p\ av}$ Mev	$(C_p + 0.2P) + .24$ cpm	C_p/P	P kw	$C_p/P(t/\rho)$
2	0	2.58	1006. ± 7	182.7 ± 1.3	5.5	88.7 ± .6
2	2	3.65	382. ± 4	69.2 ± 0.7	5.5	33.6 ± .3
3	3	4.73	398. ± 4	72.1 ± 0.7	5.5	12.6 ± .1
3	1,4	5.91	130. ± 1.5	23.4 ± 0.3	5.5	4.10 ± .05
3	3,4	6.91	52.5 ± 0.7	9.3 ± 0.1	5.5	1.63 ± .02
3	1,2,3,4	7.78	23.5 ± 0.6	4.45 ± 0.1	5.0	0.78 ± .02
4	5	9.00	25.9 ± 0.5	4.9 ± 0.1	5.0	0.233 ± .005
4	1,2,5	9.71	14.9 ± 0.4	2.7 ± 0.1	5.0	0.129 ± .004
4	2,4,5	10.91	6.58 ± 0.3	0.95 ± 0.05	5.5	0.045 ± .002
4	2,3,4,5	11.75	3.60 ± 0.2	0.41 ± 0.04	5.5	0.0195 ± .002
4	2,6	12.83	1.92 ± 0.16	0.10 ± 0.03	5.5	0.0048 ± .001
4	1,4,6	13.80	1.475 ± 0.13	0.025 ± 0.02	5.5	0.0012 ± .001
1	1,4,6	14.46	2.22 ± 0.14	0.16 ± 0.024	5.5	0.0022 ± .0004
1	1,2,3,4,6	15.48	1.36 ± 0.14	0.024 ± 0.024	5.0	0.00033 ± .0003
1	2,6	13.49	2.74 ± 0.16	0.30 ± 0.03	5.0	0.0042 ± .0004
1	3,5,6	16.65	1.41 ± 0.14	0.013 ± 0.024	5.5	0.0002 ± .0003

APPROVED FOR PUBLIC RELEASE

TABLE V

E_{p1} Mev	ΔE_p Mev	$E_{p1}+f\Delta E_p$ Mev	E_n Mev	σ_s barns	$\Delta(C_p/P\,t\rho)$ count / kw min mg/cm^2	N(E)x10^{-6} neutrons/Mev kw min	N(E)x10^{-4} neutrons/Mev kw sec
2.58	1.07	3.07	3.30	2.18	55.10 ± .7	71.7 ± .9	119.5 ± 1.5
3.65	1.08	4.15	4.46	1.75	21.0 ± .3	33.8 ± .5	56.3 ± 0.8
4.73	1.21	5.29	5.68	1.48	8.5 ± .1	14.4 ± .2	24.0 ± 0.3
5.91	1.00	6.38	6.86	1.29	2.47 ± .05	5.82 ± .1	9.7 ± 0.2
6.91	0.85	7.31	7.86	1.15	0.85 ± .03	2.64 ± .1	4.4 ± 0.2
7.78	1.22	8.34	8.97	1.03	0.547 ± .02	1.32 ± .05	2.2 ± 0.1
9.00	0.706	9.34	10.04	0.93	0.104 ± .006	0.48 ± .03	0.8 ± 0.05
9.71	1.206	10.27	11.04	0.85	0.084 ± .004	0.25 ± .01	0.42 ± 0.02
10.91	0.853	11.31	12.16	0.78	0.025 ± .003	0.117 ± .01	0.20 ± 0.02
11.75	1.065	12.25	13.17	0.72	0.015 ± .002	0.0595 ± .01	0.10 ± 0.02
12.63	0.98	13.29	14.29	0.67	0.0036 ± .001	0.017 ± .005	0.03 ± 0.01
13.49	0.98	13.95	15.00	0.64	0.0020 ± .0005	0.0097 ± .002	0.016 ± 0.003
14.46	1.01	14.93	16.05	0.59	0.0019 ± .0005	0.0096 ± .002	0.016 ± 0.003
15.48	1.155	16.01	17.22	0.54	0.0001 ± .0004	0.0005 ± .002	0.001 ± 0.003

APPROVED FOR PUBLIC RELEASE

[redacted]

TABLE VI

E	$N(E)x10^{-4}$ neutrons/Mev kw sec
3.06	6.1 ± .3
3.87	2.93 ± .1
4.73	1.50 ± .17
5.68	1.02 ± .05
6.86	0.48 ± .03
7.86	0.13 ± .04
8.80	0.11 ± .02
9.90	0.05 ± .015

[redacted]

[redacted]

The spectrum produced by the fissions in the disks alone was obtained by subtracting the values given by equation (4) from the values listed in Table V: equation (4) was assumed to hold throughout the energy range 3 - 17 Mev. Since the shape of the open hole spectrum is essentially the same as the spectrum of the beam from the multiple disk source, and constitutes only 4% of the total beam, it is believed that errors introduced by the subtraction are negligible. The difference is listed in Table VII: since wall scattering is believed to be negligible, the data listed in Table VII are believed to represent the fission spectrum.

Discussion

It is interesting to compare the observed spectrum with the predictions of the theoretical picture of the fission process. For this purpose, it is useful to combine the data of D. Hill, CP 3800, and the recent data of T. W. Bonner, R. Ferrell and W. Rinehart, LA 715, with the present data.

Hill used a proton recoil counter to observe the distribution of all neutrons (both prompt and delayed) produced in a sample of U^{235} placed in a beam of thermal neutrons. His data lie in the energy range 0.4 to 6 Mev.

Bonner et. al. used a cloud chamber filled with hydrogen at 1/3 atmosphere to observe only the prompt neutrons produced in the fission of U^{235} in a beam of thermal neutrons. They measured both the distribution in the range 0.075

[redacted]

TABLE VII

E	$N(E)x10^{4}$ multiple disk source neutrons/Mev kw sec	$N(E)x10^{-4}$* open hole neutrons/Mev kw sec	$N(E)x10^{-4}$ fission spectrum neutrons/Mev kw sec
3.30	119.5 ± 1.5	5.2	114.3 ± 1.5
4.46	56.3 ± 0.8	2.3	54.0 ± 0.8
5.68	24.0 ± 0.3	1.0	23.0 ± 0.3
6.86	9.7 ± 0.2	0.44	9.26 ± 0.2
7.86	4.4 ± 0.2	0.22	4.18 ± 0.2
8.97	2.2 ± 0.1	0.10	2.1 ± 0.1
10.04	0.8 ± 0.05	0.05	0.75 ± 0.05
11.04	0.42 ± 0.02	0.025	0.40 ± 0.02
12.16	0.20 ± 0.02	0.01	0.18 ± 0.02
13.17	0.10 ± 0.02	0.006	0.094 ± 0.02
14.29	0.03 ± 0.01	0.003	0.027 ± 0.01
15.00	0.016 ± 0.003	0.0016	0.014 ± 0.003
16.05	0.016 ± 0.003	0.0008	0.015 ± 0.003
17.22	0.001 ± 0.003	0.00035	0.001 ± 0.003

* see text

APPROVED FOR PUBLIC RELEASE

to 0.6 Mev, and the relative number of proton recoils above and below 0.6 Mev. The composite spectrum so obtained extends from 0.075 to 17 Mev; it is believed that the normalization constants are correct within 10%, and at neither of the two joins was there a detectable difference in the slopes.

The first formula tried for fit was that developed by Feather in BM 148. The three basic assumptions used were: (1) Isotropic emission in the center of mass system of fragment and neutron; (2) Neutron distribution in the c.m. system proportional to $E\, e^{-E/Q}$; (3) Fragment velocity corresponding to the full kinetic energy.

The first assumption was made largely for its simplicity and for lack of other knowledge. The second assumption is based on the expected distribution of particles from a liquid drop model of the fragment. The third is based on the expectation that the neutron leaves the fragment in a time of the order 10^{-15} second after the fragments separate; from the range energy relation deduced for such fragments, it is calculated that the fragment loses a negligible fraction of its original energy in that time, though several collisions may have occurred. If the emission time is an order of magnitude longer or the specific ionization higher at the start of the track the assumption is invalid, so must be considered suspect.

Attempts to find values for the two constants (Q and the product $E_f m/M$, where E_f is the fragment's kinetic

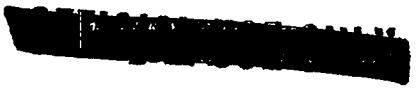

energy at the time of neutron emission and m and M are the masses of the neutron and fragment, respectively) appearing in the equation assuming one average fragment were unsuccessful. The curve computed from the assumption of two fragments, one having the average energy and mass of the light group and the other the energy and mass of the heavy group, is shown in comparison with the composite curve in Fig. 4.

S. de Benedetti, J. E. Francis, W. M. Preston, and T. W. Bonner performed an experiment to determine the angular correlation of the neutrons produced. Their data indicate that the neutrons leave rapidly moving fragments, or that there is a very improbable angular correlation between the neutrons after the fragments are stopped. Assuming the full kinetic energy, they concluded that the number of fissions where one neutron leaves each fragment are at least twice as numerous as the fissions where a pair of neutrons leave the same fragment. The light and heavy groups of fragments must then contribute nearly equal numbers of neutrons. This fact was used to determine the relative intensities of the two groups of neutrons.

The fit was regarded as unsatisfactory, implying the failure of at least one of the three assumptions. Rather laborious calculations are necessary to determine the spectrum given by Feather's formula, so no attempt was made

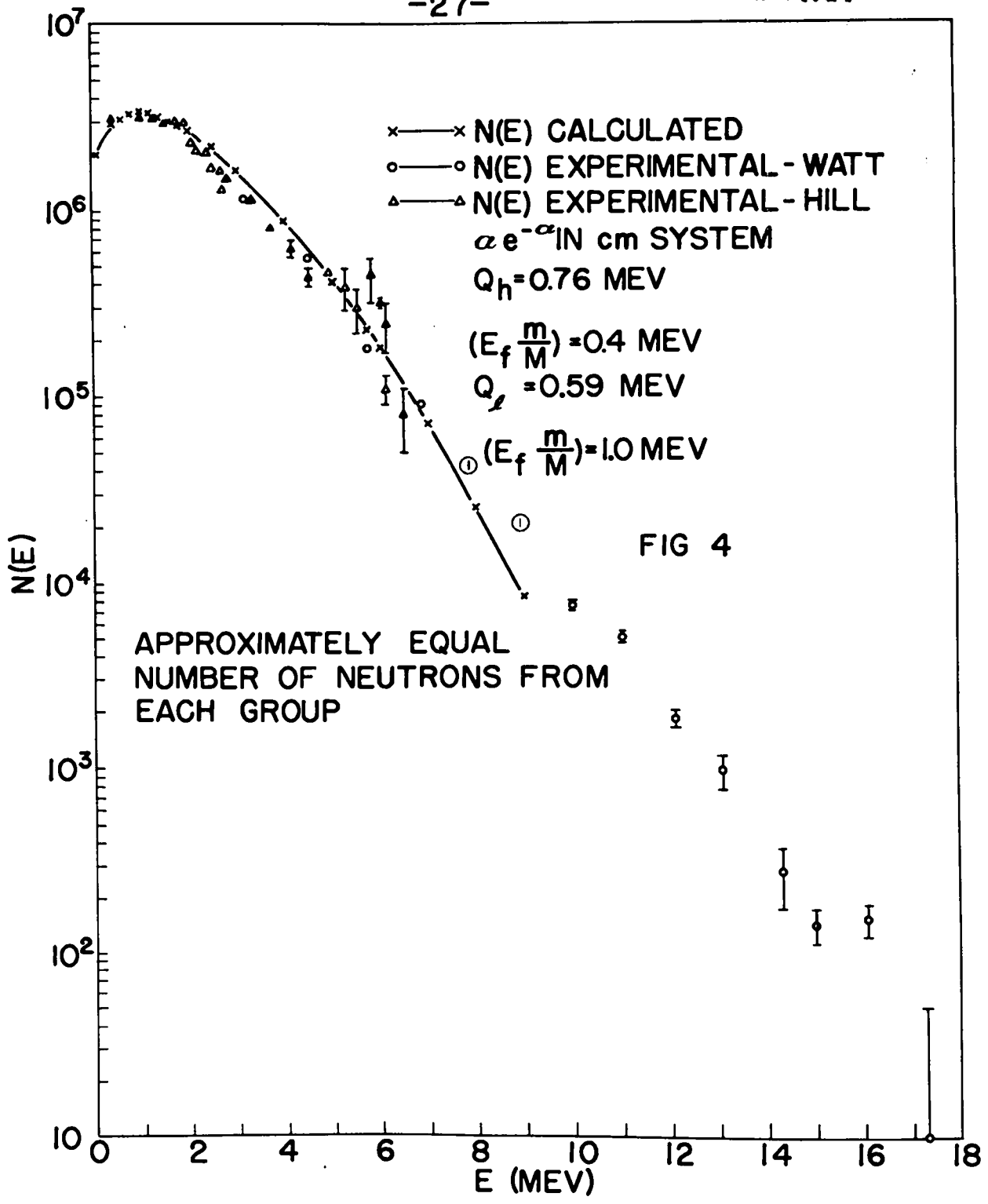

FIG 4

[redacted]

to add the spectra of a large number of fragments; general indications are that a better fit could be obtained by assuming that the fragments (particularly the light group) had less than half their original kinetic energy when the neutron was emitted.

It is interesting to note that a simple formula giving quite acceptable fits is obtained by assuming a Maxwellian distribution ($E^{\frac{1}{2}} e^{-E/Q}$) in place of assumption (2) above. The resulting formula is

$$N(E) = \text{const} \times \sinh 2(EE_fm/M)^{\frac{1}{2}}/Q \quad e^{-E/Q} \qquad (5)$$

Assuming only one fragment, acceptable fits are obtained with several sets of the constants Q and (E_fm/M) which are to some extent interrelated. Partly because of the simplicity of the resulting equation, the values $Q = 1.00$ Mev and $E_fm/M = 0.5$ Mev were chosen as best representing the data. The formula is then

$$N(E) = 4.75 \times 10^6 \sinh (2E)^{\frac{1}{2}} e^{-E} \qquad (6)$$

Equation (6) and the data are plotted in Fig. 5.

In order to see if equation (5) could be made to give an acceptable fit when the spectra from the two groups were added, two such terms, in which the products (E_fm/M) were set equal to the averages for the heavy and light groups, 0.41 and 0.92, respectively. As a second condition,

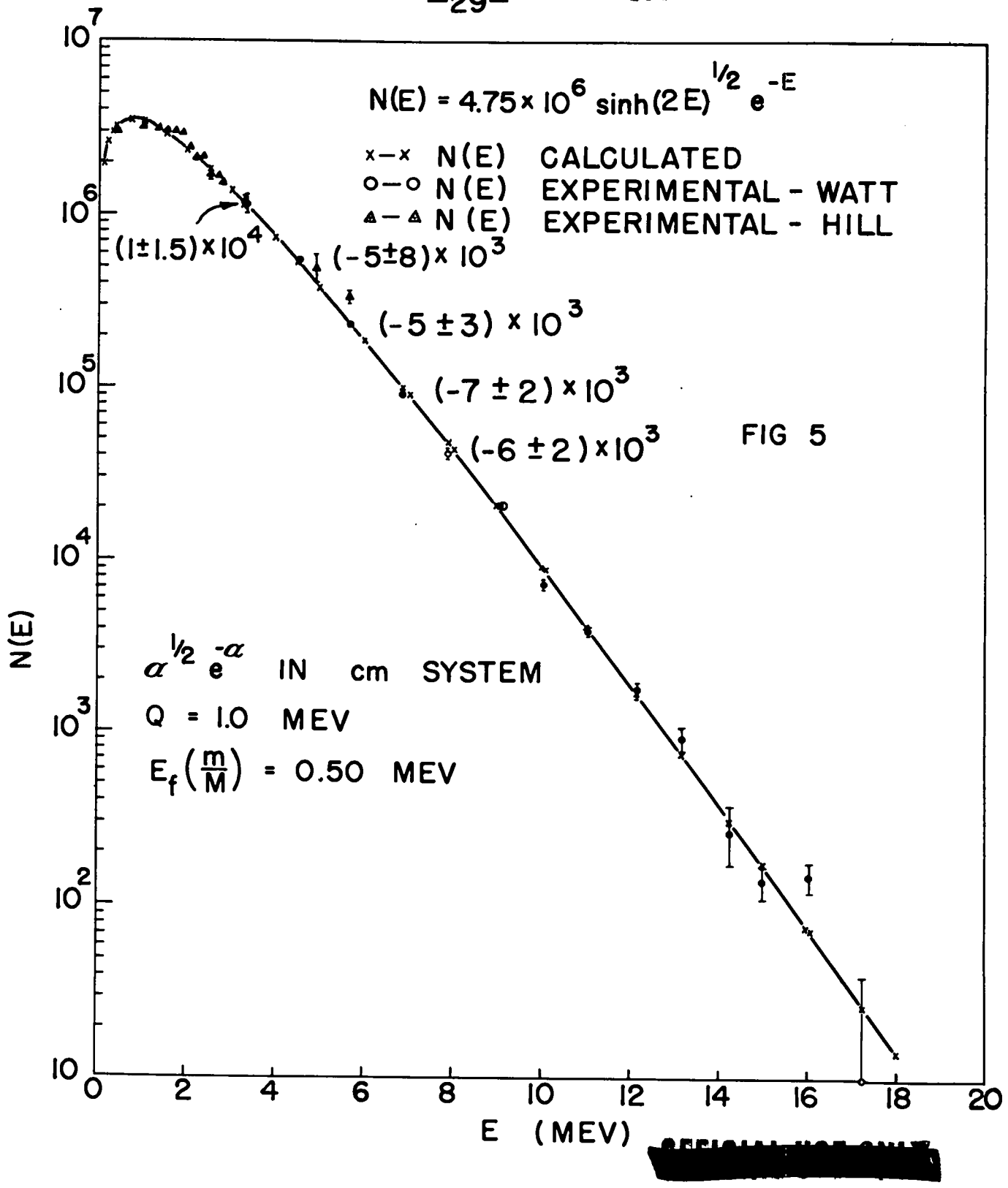

the number of neutrons from each group were set equal, and, as a third, the values of constants (λ) were set equal. The absolute value of Q is then the only remaining arbitrary constant (except the normalization constant needed to fit any particular set of data), and was determined from the slope of the data in the region around 9 Mev. The resulting equation is

$$N(E) = 1.088 \times 10^6 \sinh 1.92(E)^{\frac{1}{2}} e^{-E/0.875} + 2.937 \times 10^6 \sinh 1.28(E)^{\frac{1}{2}} e^{-E/0.875} \quad (7)$$

A plot of equation (7) and the data is given in Fig. 6.

In both Fig. 5 and 6 the equations show downward curvature, while the data fall more nearly on a straight line. The deviation of the data is of the same order of magnitude as the systematic error expected from the arbitrary join in the curves used for the (n,p) scattering cross section, so can't be taken as real. To explore the implications of a real deviation like that observed, and to find an equation giving a fit passing more nearly through all points, the conditions of equal number from each group and equal Q for each group were abandoned.

The downward curvature of the calculated spectra can be removed by assuming different Q's for the two groups, and several cases were calculated. Three cases thought to give the best of the acceptable fits are plotted in Figs.

[redacted]

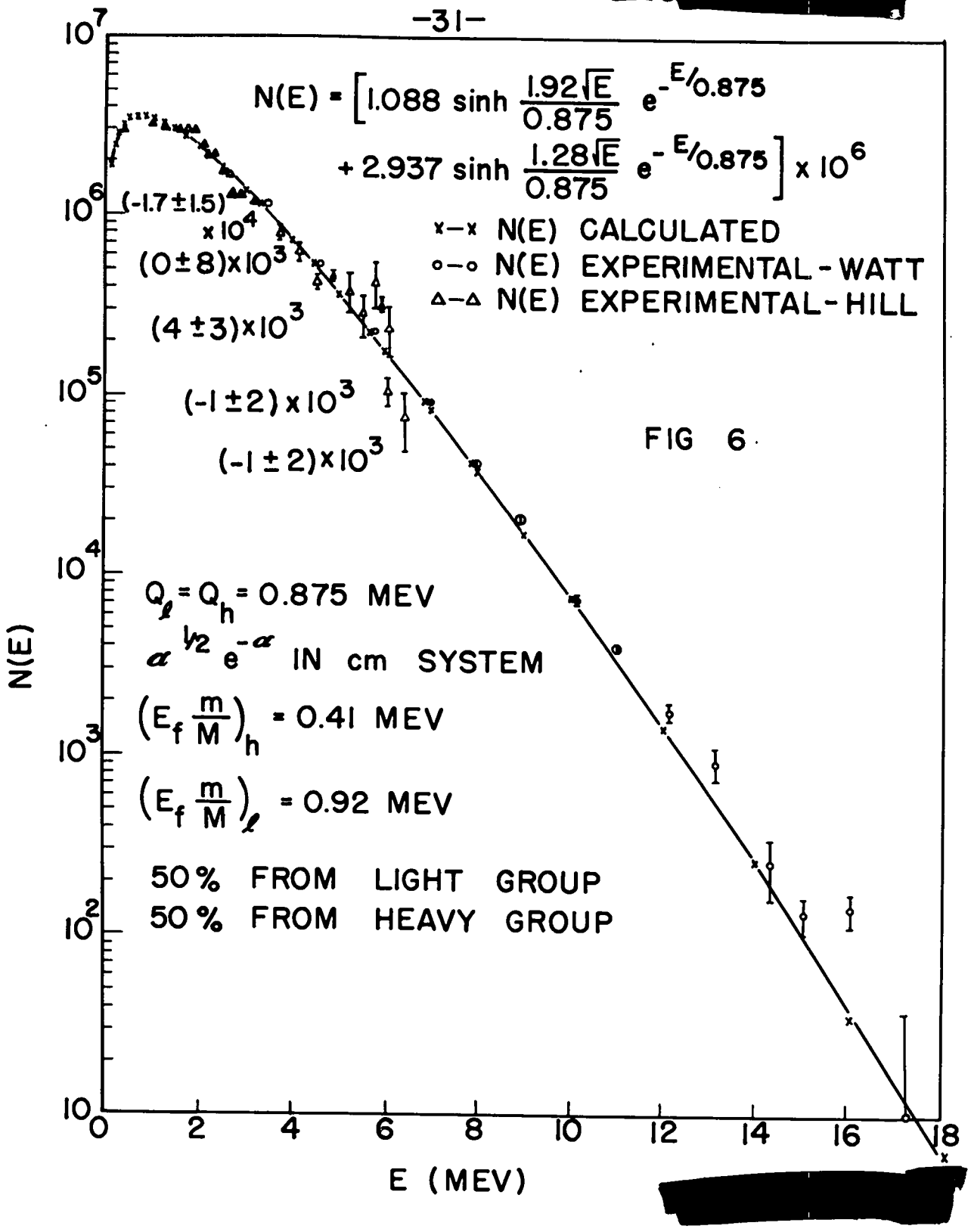

FIG 6

[redacted]

7, 8, and 9; the values used for the Q's and the contribution from each group are shown in the Figures.

[redacted]

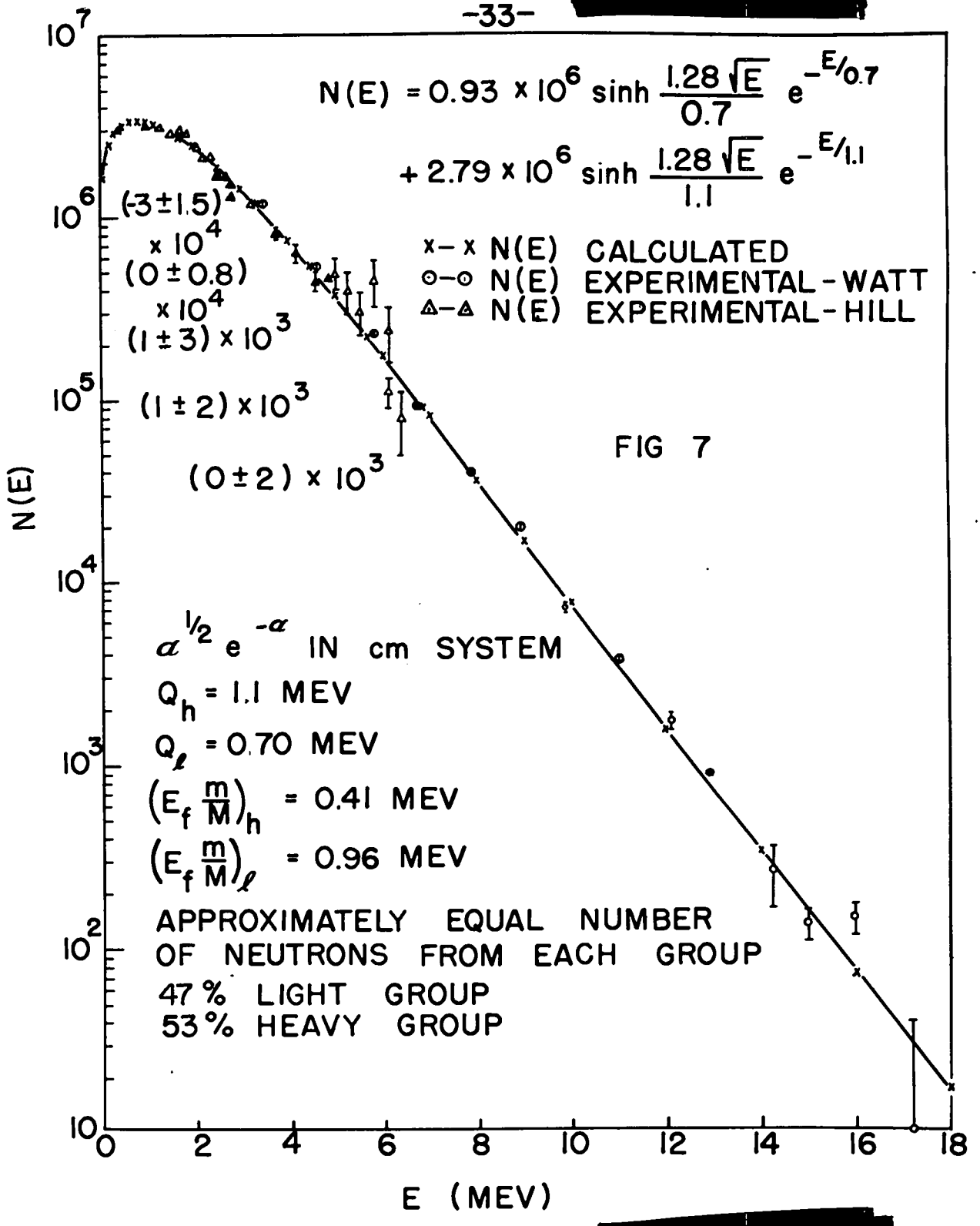

[redacted]

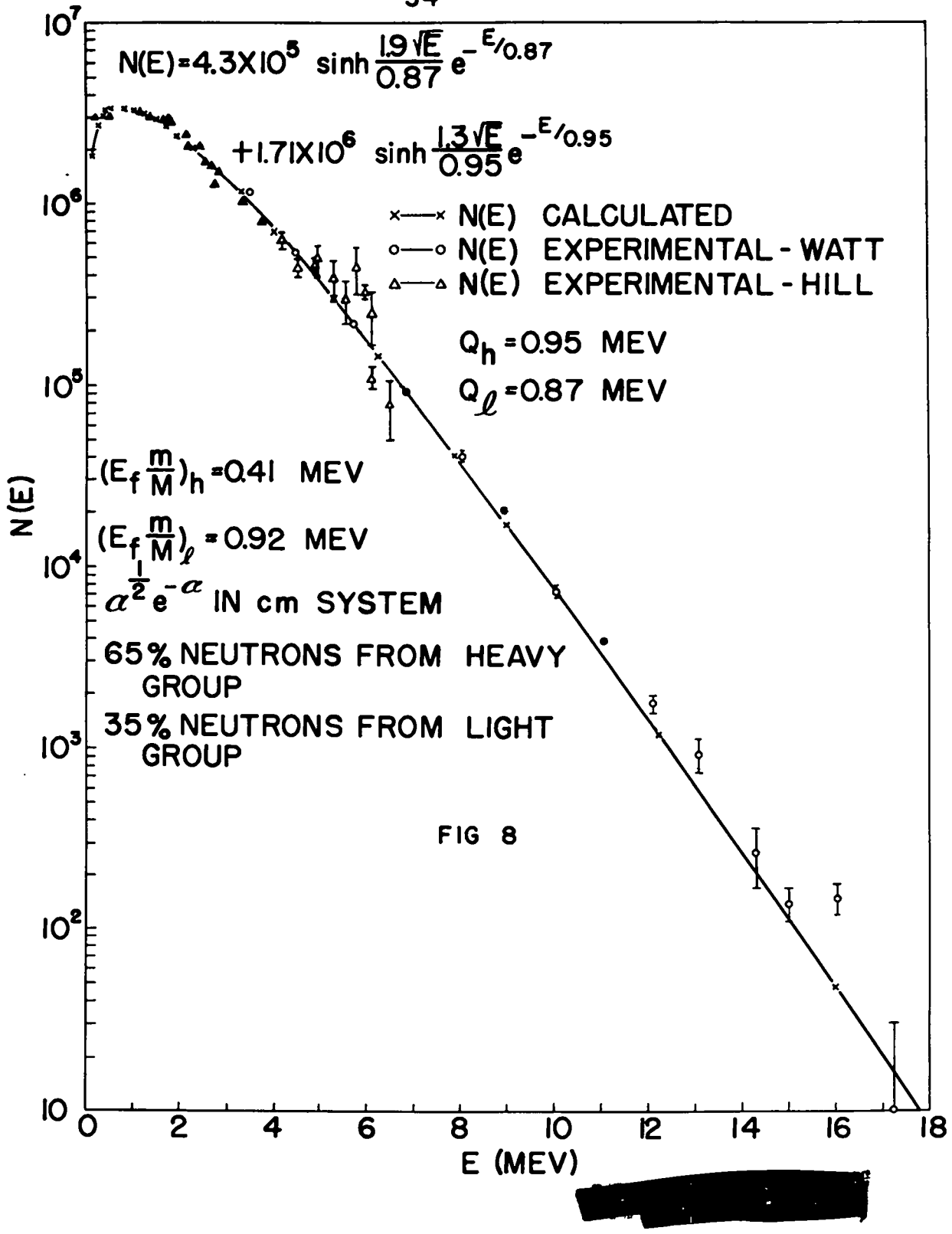

FIG 8

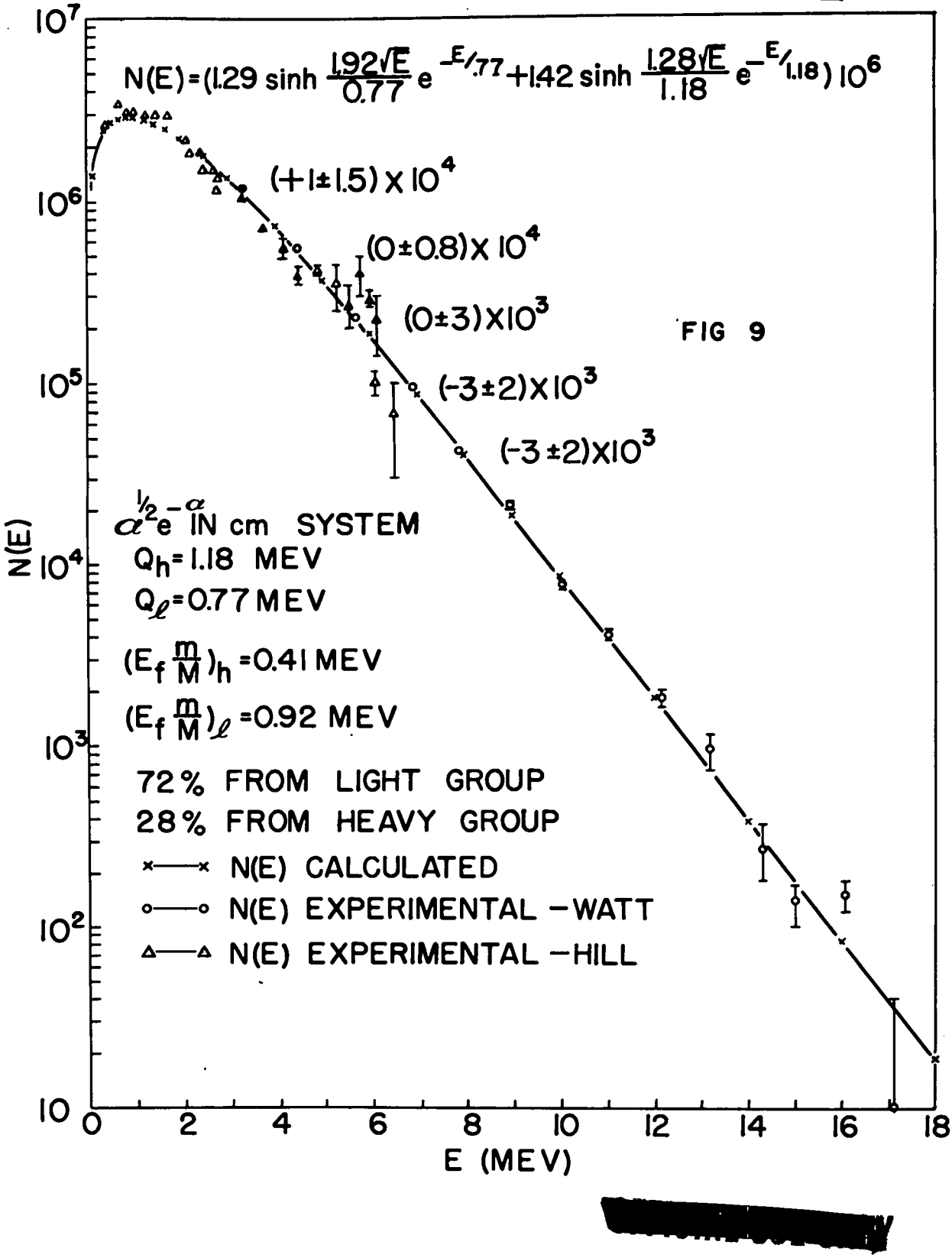

FIG 9

[redacted]

APPENDIX I

E	$-\frac{dE}{dx}$	R
Mev	$\frac{\text{Mev}}{\text{mg/cm}^2}$	mg/cm^2
1		3.45
1.5		6.69
2	11.5×10^{-2}	10.8
2.5	9.85	15.6
3	8.62	21.0
3.5	7.69	27.3
4	6.96	34.5
4.5	6.37	42.1
5	5.88	50.3
5.5	5.47	59.0
6	5.12	69.1
6.5	4.82	79.2
7	4.55	90.0
7.5	4.31	101.3
8	4.10	113.2
8.5	3.92	125.6
9	3.75	138.8
9.5	3.59	152.4
10	3.45	166.7
10.5	3.32	181.4
11	3.21	196.6
11.5	3.10	212.5
12	2.99	229.0
12.5	2.90	246.1
13	2.816	263.7
13.5	2.734	281.8
14	2.658	300.6
15	2.518	339.3
17	2.281	422.8
19	2.089	514.6
21	1.930	614.3

The curves shown in Fig. 10 were used to interpolate between the tabulated values.

[redacted]

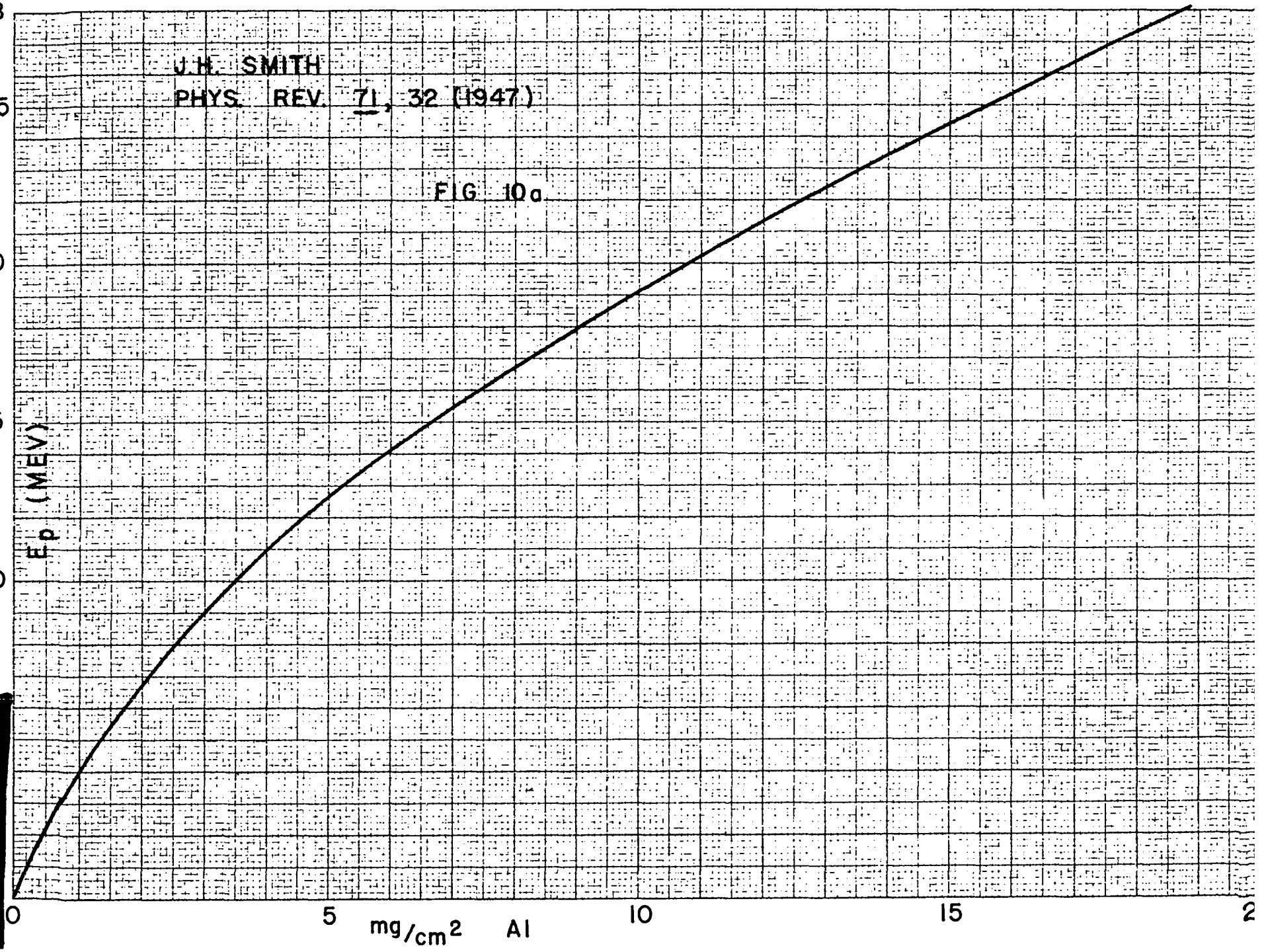

APPROVED FOR PUBLIC RELEASE

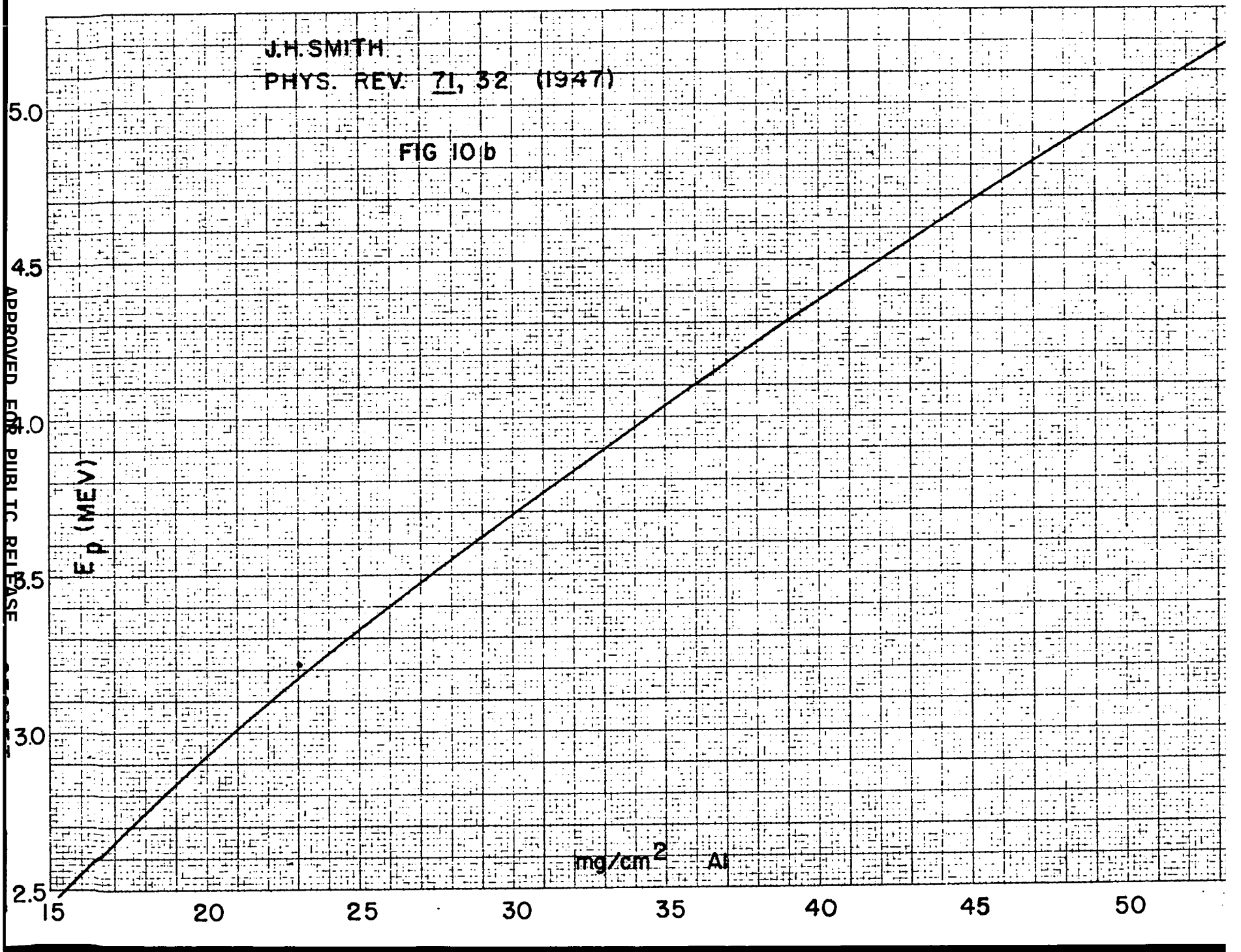

APPROVED FOR PUBLIC RELEASE

J.H. SMITH

PHYS. REV. 71, 32 (1947)

FIG 10c

APPROVED FOR PUBLIC RELEASE

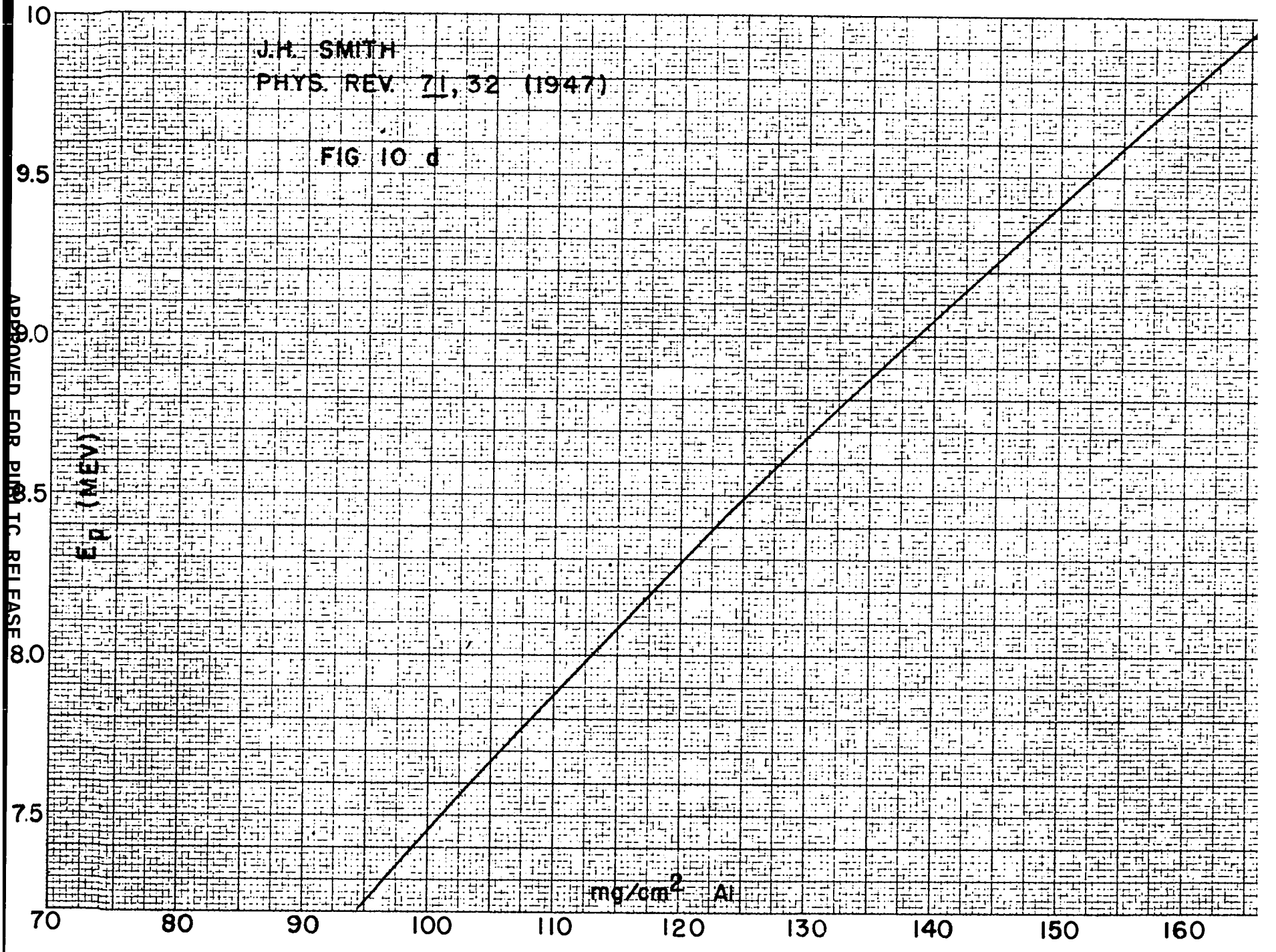

APPROVED FOR PUBLIC RELEASE

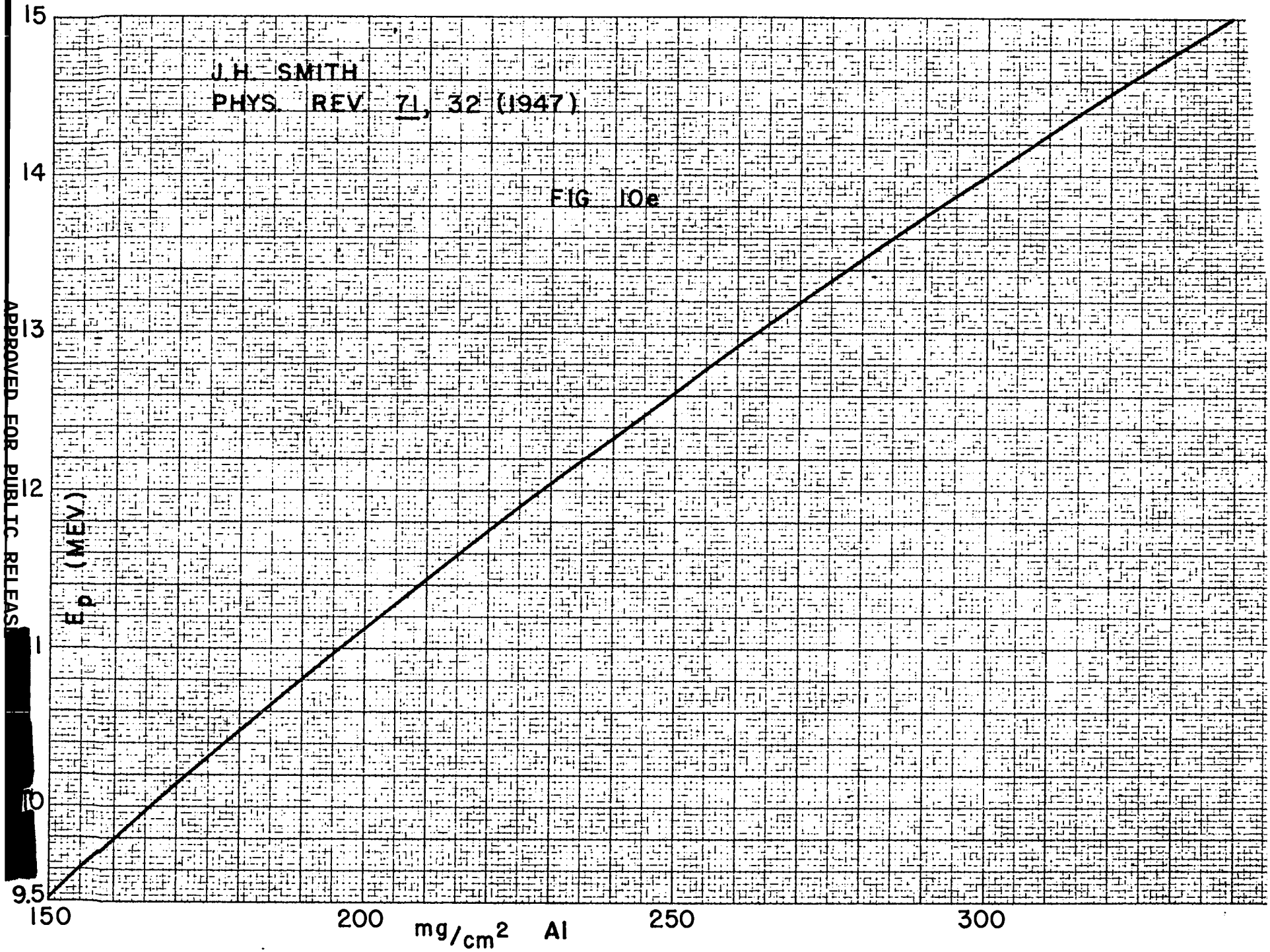

APPROVED FOR PUBLIC RELEASE

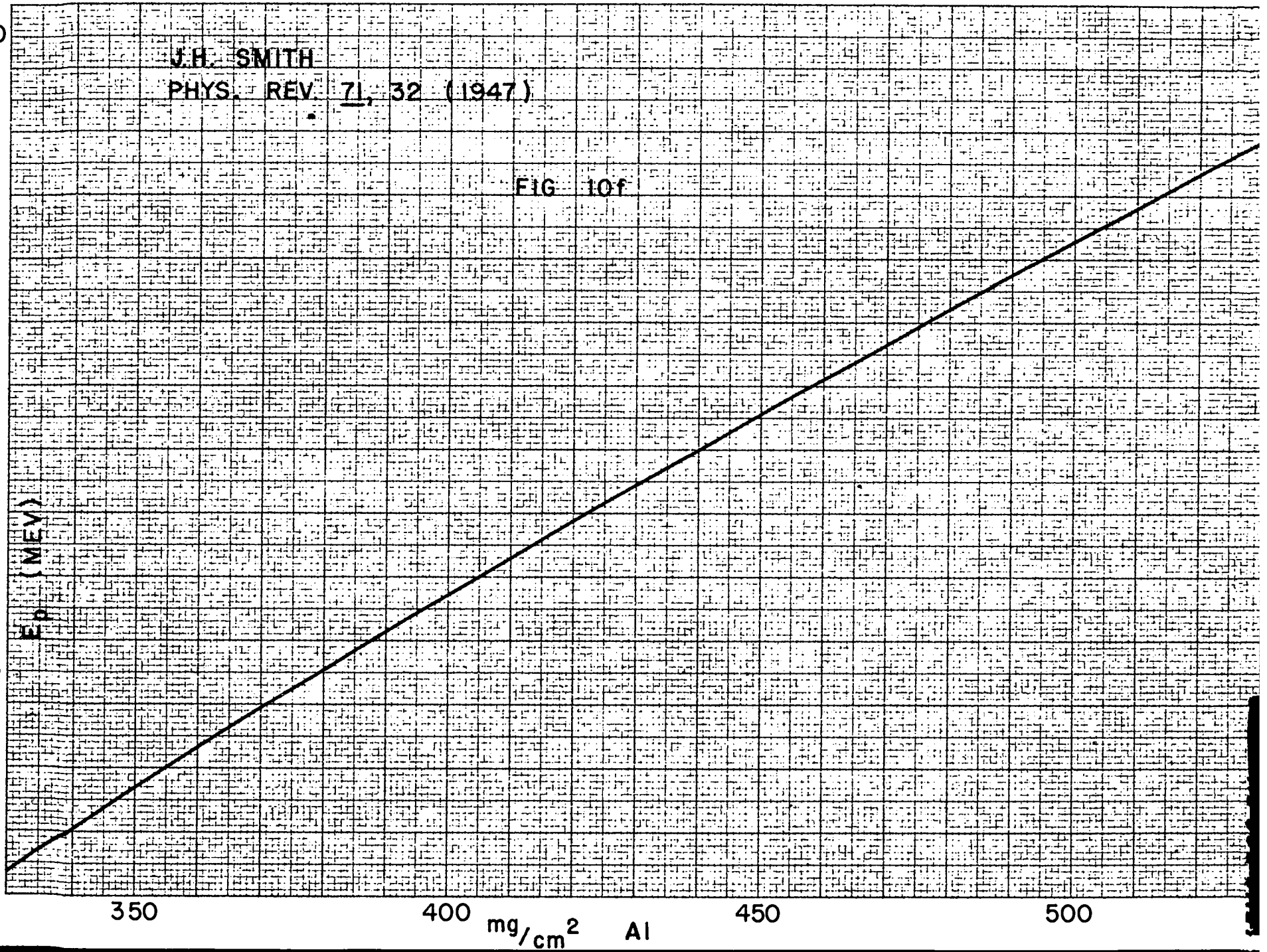

APPROVED FOR PUBLIC RELEASE

APPENDIX II

Scattering cross section for neutrons by protons.

The formula developed by Bohm and Richman, Phys. Rev., 71, 570 (1947), and the formula developed by Louis Goldstein, LA-702, are plotted in Fig. 11, together with the data of Bailey, Bennett, Bergstrahl, Nuckolls, Richards and Williams, Phys. Rev., 70, 583 (1946), R. Sherr, Phys. Rev., 68, 240 (1945) and W. Sleator, Jr., Phys. Rev., 72, 207 (1947).

The values used in the computation of the fission spectrum are listed in the table.

TABLE

E	σ_s	E	σ_s
3.06	2.31	8.80	1.05
3.30	2.18	8.97	1.03
3.87	1.91	9.90	0.94
4.46	1.75	10.04	0.93
4.73	1.69	11.04	0.85
5.68	1.48	12.16	0.78
6.86	1.29	13.17	0.72
7.86	1.15	14.29	0.67
		15.00	0.64
		16.05	0.59
		17.22	0.54

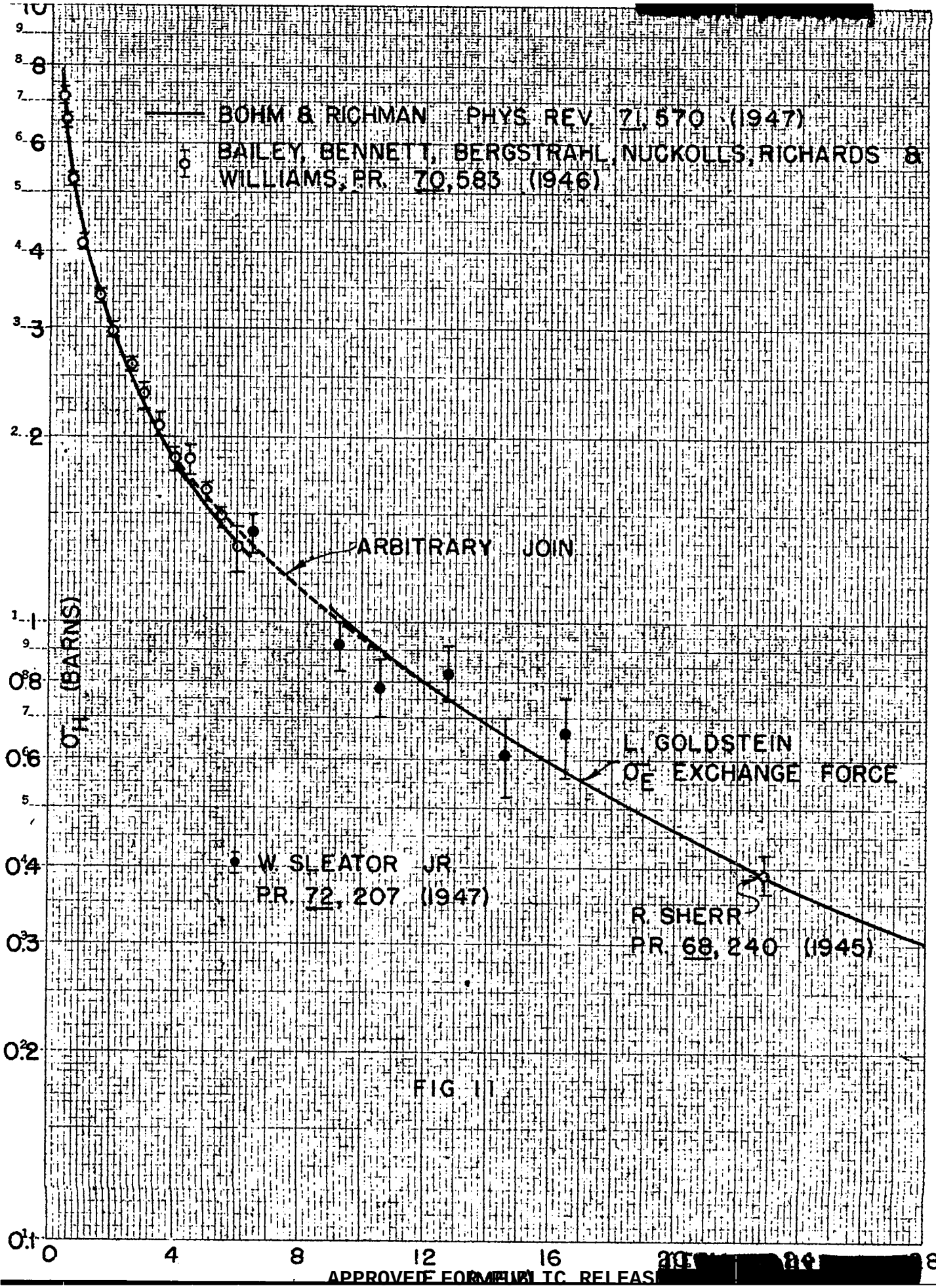

FIG 11

APPENDIX III

The calculations leading to the number of neutrons required to produce a particular proton recoil counting rate are separable into (1) the probability that a particular neutron will produce a proton recoil and (2) the probability that the proton will enter the counters.

Owing to the 15.5° inclination of the spectrometer, the neutron path in the polyethylene has a length $t/\cos 15.5^{\circ} = t/0.964$. The polyethylene has a composition not appreciably different from $(CH_2)_x$, hence the number of protons/milligram of polyethylene is given by $2/14.026 \times 6.02 \times 10^{20} = 8.58 \times 10^{19}$.

The number of protons/(cm^2 normal to neutron path) is then found to be

$$(t/0.964) \times \rho \times 8.58 \times 10^{19} = 8.90 \times 10^{19} \ (t\rho)$$

where t is the thickness of the polyethylene normal to its own surfaces and ρ is its density (milligrams/cm^3).

The projected area of all the protons is then $8.90 \times 10^{19} \ (t\rho)\sigma_s$, where σ_s is the proton scattering cross section in cm^2: where σ_s is in barns, the projected area is $8.90 \times 10^{-5} \ (t\rho) \ \sigma_s$.

In these experiments, the largest value used for the product $(t\rho) \ \sigma_s$ was $\simeq 0.07$, so the projected

area was $\simeq 6 \times 10^{-3}$ cm^2/cm^2 of beam.

The scattering probability was therefore taken to be the projected area/cm^2 of beam, with a maximum error of 0.6%. Then

$$P_s = 8.90 \times 10^{-5} (t\rho)\, \sigma_s \qquad (1)$$

In computing the probability that a proton recoil will enter the counters, the (n,p) scattering was assumed to be isotropic in the center of mass system. The error introduced by this simplification is probably less than 10% at 14 Mev, and smaller at lower energies.

By the usual transformation from the laboratory system to the center of mass (c.m.) system, the solid angles are found to be given by

$$d W_{cm} = 4 \cos\theta \; dW_{lab}$$

$$W_{cm} = 4 \overline{\cos\theta} \; W_{lab}$$

where $\cos\theta$ is the lab angle (from the forward direction) of the element of solid angle $d W_{lab}$. The average value of $\cos\theta$ was taken to be that at the center of the counter window, $\cos 15.5^\circ = 0.964$.

The counter window was 1.2" in diameter and 10.05" from the polyethylene source. The half-angle (β) of the cone was then found from

$$\tan\beta = 0.60/10.05 = 0.0597$$

$$\beta = 3^\circ 25'$$

The solid angle subtended is then

$W_{lab}/4\pi = 1-\cos\beta/2 = 1-0.99822/2 = 0.00089$

and

$$W_{cm}/4\pi = 4 \times 0.964 \times 8.9 \times 10^{-4} = 3.44 \times 10^{-3} \qquad (2)$$

The ratio $(W_{cm}/4\pi)$ is taken to be the probability that the proton will enter the counters.

The probability that a neutron will give a count is then the product of (1) and (2), whence

$$d N_p = dN_n \left[8.90 \times 10^{-2} \times 3.44 \times 10^{-3} \sigma_s (t\rho)\right]$$
$$= dN_n \, 30.62 \times 10^{-8} \, \sigma_s (t\rho) ,$$

or

$$dN_n = dN_p \times \left(3.27 \times 10^6 / \sigma_s (t\rho)\right) \qquad (3)$$

(σ_s in barns, $(t\rho)$ in mg/cm^2).

Assuming that the protons can penetrate into the counters and that they have 100% efficiency.

Define:

C_p = proton counting rate = number of protons penetrating counters/minute;

P = "Water Boiler" power, kw, proportional to source strength;

$P\,N_p = dN_p/dE_p$ = (number of protons having energy between E_p and $E_p + dE_p$)$/dE_p$;

$P\,N_n = dN_n/dE_n$ = (number of neutrons in beam having energy between E_n and $E_n + dE_n$)$/dE_n$.

Then

$$C_p = P \int_{E_{av}}^{\infty} N_p \, dE_p$$

where E_{av} is the average minimum energy of the protons capable of giving a count.

The difference between the counting rates observed for different absorber combinations, therefore different E_{av}, is

$$\Delta C_p = P \int_{E_{av\ 1}}^{E_{av\ 2}} N_p \, dE_p$$

Then

$$N_p(E^*) = \Delta C_p / P \Delta E_p$$

where $\Delta E_p = (E_{av\ 2} - E_{av\ 1})$

and $E^* = (E_{av\ 1} + f \Delta E_p)$.

The value of f depends on the distribution function, and is derived in Appendix IV .

From the definitions,

$$dN_n = N_n \, dE_n \ , \ dN_p = N_p \, dE_p$$

and from the probabilities considered above,

$$dN_n = \left(3.27 \times 10^6 / \sigma_s \, (t\rho)\right) dN_p$$

$$N_n = \left(3.27 \times 10^6 / \sigma_s \, (t\rho)\right) N_p \, (dE_p/dE_n)$$

Also, from the conservation laws

$$E_p = E_n \cos^2 \theta$$

The mean angle, (15.5°), was used, giving

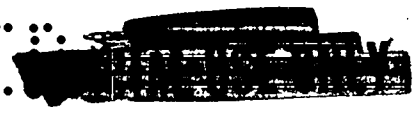

$$E_p = E_n \cos^2 15.5^\circ = 0.93\, E_n$$

Then

$$N_n = N_p \left(3.04 \times 10^6 / \sigma_s\, (t\rho)\right)$$

$$N_n = 3.04 \times 10^6 \frac{(C_p/Pt\rho)}{\sigma_s\, \Delta E_p} \qquad (4)$$

$$E_n = (E_{av\ 1} + f\, \Delta E_p)/0.93 \qquad (5)$$

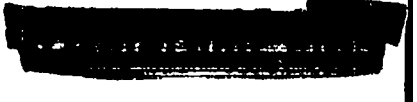

APPENDIX IV

Take the neutron distribution of the form

$$N(E) = K\, e^{-E/Q}$$

The average value in the interval $E_1 \rightarrow E_2$ is found to be

$$\overline{N(E)} = K \int_{E_1}^{E_2} e^{-E/Q}\, dE \quad / \Delta E \qquad \Delta E = E_2 - E_1$$

$$= \frac{KQ}{\Delta E} \left(e^{-E_1/Q} - e^{-E_2/Q}\right)$$

$$= \frac{KQ}{\Delta E}\, e^{-E_1/Q} \left(1 - e^{-\Delta E/Q}\right)$$

Define f as the fraction of the interval ΔE where the function takes on the average value; then

$$\overline{N(E)} = K\, e^{-(E_1 + f\Delta E)/Q} = \frac{KQ}{\Delta E}\, e^{-E_1/Q} \left(1 - e^{-\Delta E/Q}\right)$$

$$e^{-f\Delta E/Q} = \left(1 - e^{-\Delta E/Q}\right) Q/\Delta E$$

$$f = (Q/\Delta E)\, \ln(\Delta E/Q) - (Q/\Delta E)\, \ln\left(1 - e^{-\Delta E/Q}\right)$$

The value of f is plotted in Fig. 12.

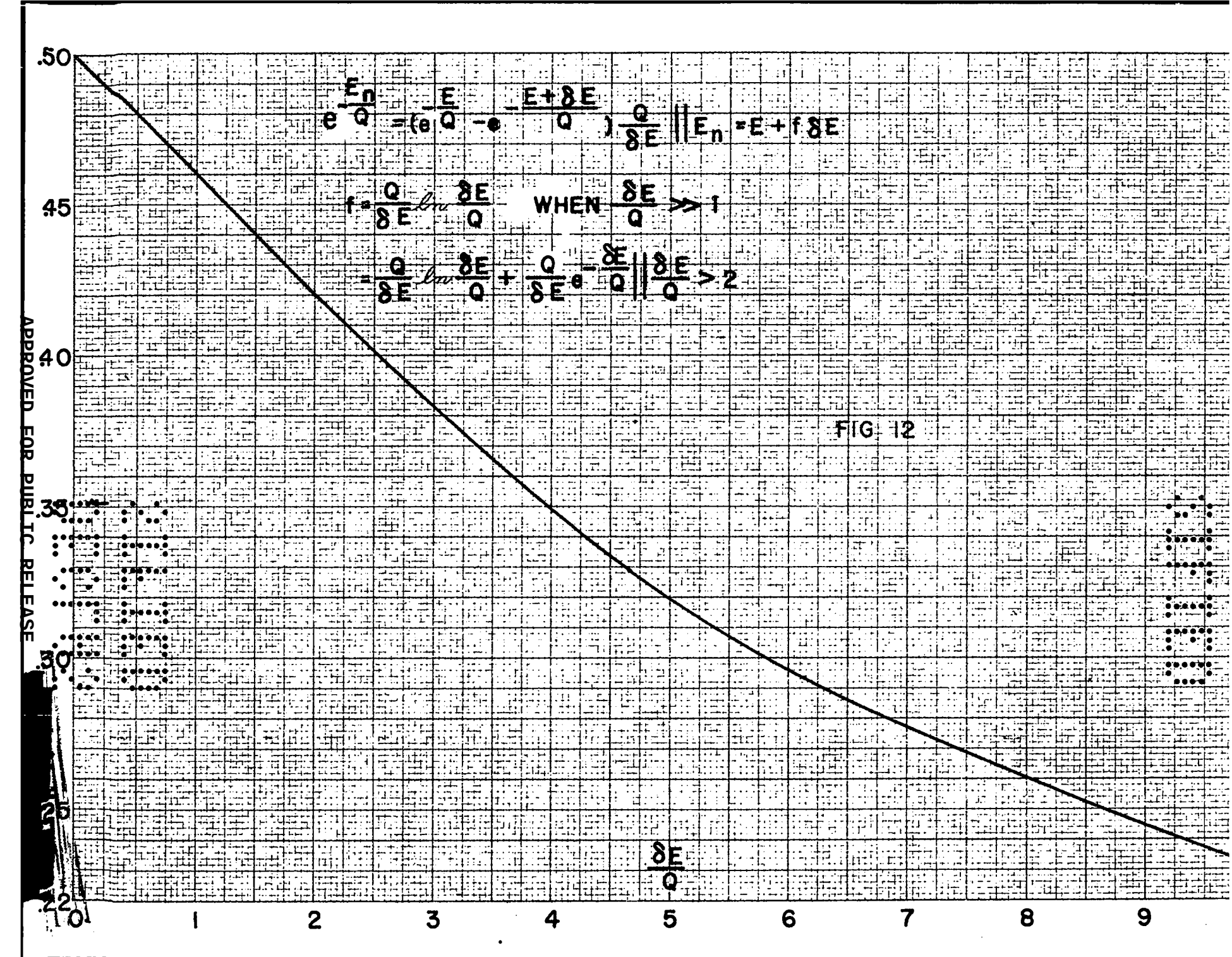

APPROVED FOR PUBLIC RELEASE

UNCLASSIFIED

UNCLASSIFIED